ENVIRONMETRICS
Environmetrics 2005; **16**: 573–587
Published online 21 April 2005 in Wiley InterScience (www.interscience.wiley.com). DOI: 10.1002/env.723

Mapping sea bird densities over the North Sea: spatially aggregated estimates and temporal changes

Edzer J. Pebesma[1]*,†, Richard N. M. Duin[2] and Peter A. Burrough[1]

[1]*Faculty of Geosciences, Department of Physical Geography, Utrecht University, P.O. Box 80.115, 3508 TC Utrecht, The Netherlands*
[2]*Dutch National Institute for Coastal and Marine Management (RIKZ), P.O. Box 20907, 2500 EX Den Haag, The Netherlands*

SUMMARY

In the Dutch sector of the North Sea, sea bird densities are recorded bi-monthly by using airborne strip-transect monitoring. From these data we try to estimate: (i) high-resolution spatial patterns of sea bird densities; (ii) low-resolution spatial-average bird densities for large areas; and (iii) temporal changes in (i) and (ii), using data on *Fulmaris glacialis* as an example. For spatial estimation, we combined Poisson regression for modelling the trend as a function of water depth and distance to coast with kriging interpolation of the residual variability, assuming spatial (co)variances to be proportional to the trend value. Spatial averages were estimated by block kriging. For estimating temporal differences we used residual cokriging for two consecutive years, and show how this can be extended to analyse trends over multiple years. Approximate standard errors are obtained for all estimates. A comparison with a residual simple kriging approach reveals that ignoring temporal cross-correlations leads to a severe loss of statistical accuracy when assessing the significance of temporal changes.This article shows results for *Fulmaris glacialis* monitored during August/September in 1998 and 1999. Copyright © 2005 John Wiley & Sons, Ltd.

KEY WORDS: generalized linear models; Poisson regression; kriging; cokriging; block kriging; spatial aggregation; *Fulmaris glacialis*

1. INTRODUCTION

The Dutch sector of the North Sea (NCP) is an important habitat for several sea bird species. In 1984, the Dutch National Institute for Coastal and Marine Management (RIKZ) started a programme for the systematic airborne monitoring of sea birds over the NCP. At present, the monitoring programme is carried out bi-monthly. The main aim of this programme is to obtain information about the spatial distribution of sea bird density and temporal changes in spatial patterns. The actual observations cover less than 0.5% of the total area, and statistical estimation is needed to fill in the gaps.

*Correspondence to: E. J. Pebesma, Faculty of Geosciences, Department of Physical Geography, Utrecht University, P.O. Box 80.115, 3508 TC Utrecht, The Netherlands.
†E-mail: e.pebesma@geog.uu.nl

Received 23 February 2004
Accepted 1 November 2004

When estimating spatial patterns, there is a well-known trade-off between spatial resolution and statistical estimating accuracy (Pebesma and de Kwaadsteniet, 1997; Heuvelink and Pebesma, 1999): either high-resolution spatial predictions can be made that have a low statistical accuracy (large estimation errors), or low-resolution estimates for large areas can be made with usually a much higher statistical accuracy. In other words: given a certain amount of measurements, to increase statistical accuracy, spatial resolution has to be sacrificed. Both low-resolution and high-resolution approaches may, however, yield valuable results: the high-resolution spatial predictions may give us the most detail about *where* the highest or lowest densities are expected, whereas the low-resolution estimates can be used to accurately assess average densities (or total numbers of birds) for sensibly chosen larger areas. In this article we compare both, and we will also look at temporal changes in sea bird densities, both for high-resolution spatial patterns and for low-resolution estimates.

2. DATA

2.1. External variables

For the estimation of spatial distribution of birds, we would ultimately like to know why birds prefer to be in specific areas. Outside the breeding season, a major motivation seems to be the presence of food. If we then knew the abundance of the food for given bird species everywhere on the NCP, this information would be very valuable to predict bird densities. Variables that were available in this study and that may serve as proxies to food conditions are distance to the (Dutch) coast and water depth (Figure 1). These variables may be relevant when predicting densities of species that prefer shallow water/near coast conditions, or deep water/open sea conditions, or other combinations.

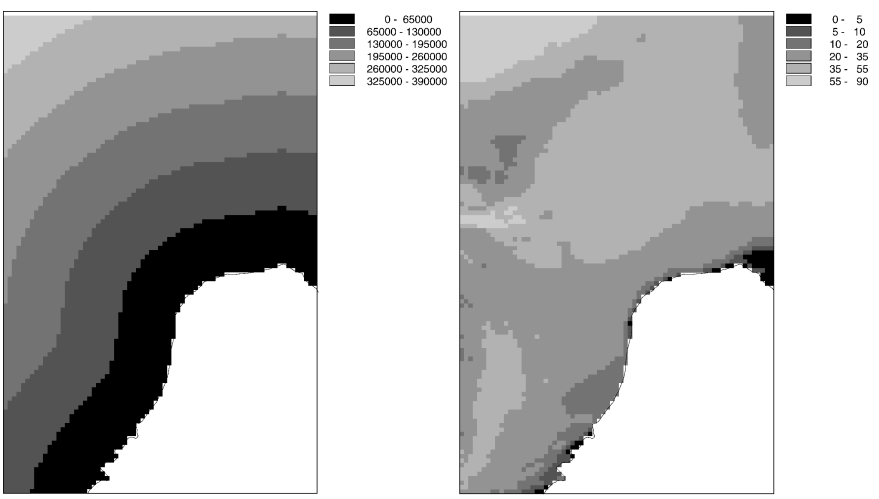

Figure 1. (a) Distance to coast (m); (b) sea water depth (m)

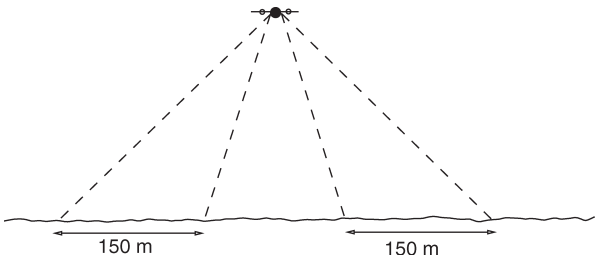

Figure 2. Schematic representation of the airborne monitoring. Flight height is 170 m (500 ft, the minimum allowed); depending on light and wave conditions, monitoring takes either place on both sides or on one side

2.2. *Sea birds*

Sea bird data are collected as strip transect counts, using bi-monthly airborne monitoring. Ideally, the samples for the NCP are taken within three subsequent days. During the monitoring flights, depending on light and wave conditions either on one or on both sides of the plane, birds visible within a strip of approximately 150 m width are registered for fixed time periods of approximately 1 min (Figure 2). This corresponds to a strip length of approximately 3 km, approximately resulting in a 0.5 km^2 single observation area. For a given species a single 'observation' therefore does not correspond to the observation location of single birds, but to the number of birds observed within a strip that has a known location and size. Location and size are derived from observation time, flying speed and flight plan co-ordinates. An example of observed densities for *Fulmaris glacialis* (Fulmar) is shown in Figure 3. Bird counts are transformed to bird densities by dividing each count through the corresponding observation area.

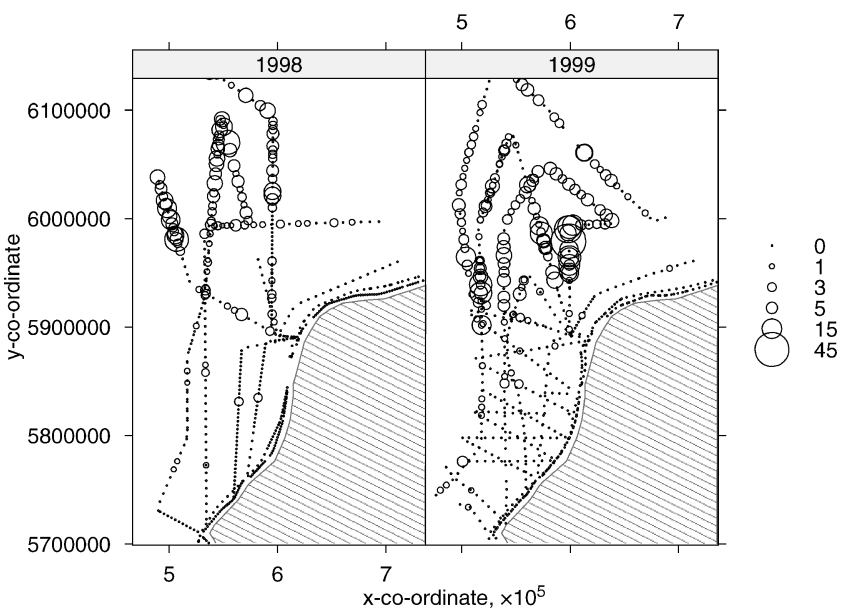

Figure 3. Observed densities of *Fulmaris glacialis* during the August/September monitoring of 1998 and 1999 (km^{-1}); co-ordinates are in UTM31. The shaded area is a generalized (outer) coastline

3. SPATIAL PREDICTION

Although strictly speaking the observations of sea bird densities are taken from a space–time process $y(s,t)$, with s and t the continuous space and time co-ordinate, the monitoring programme aims at collecting data at fixed moments in a year, and we will write them as $y_t(s)$, stressing that t is an index. In this study the t subscript always refers to either August/September 1998 or August/September 1999, which we will abbreviate to $t \in \{98, 99\}$.

For mapping bird densities, the variability of the measurements $y_t(s)$ is modelled by a structural component, the trend $\mu_t(s)$, and a random component, the residual $e_t(s)$:

$$y_t(s) = \mu_t(s) + e_t(s), \quad s \in \{s_{1,t}, \ldots, s_{n_t,t}\},\ t \in \{98, 99\} \tag{1}$$

with $s_{1,t}, \ldots, s_{n_t,t}$ the n_t data locations of year t. Mapping involves the spatial prediction of $y_t(s_0)$ at any (unobserved) location s_0 and observed time $t \in \{98, 99\}$, or the prediction of the spatially aggregated (averaged) value of y_t over an area B_0, $y_t(B_0) = \frac{1}{|B_0|}\int_{B_0} y_t(u)\,\mathrm{d}u$ with $|B_0|$ the area of B_0. For this, we need suitable models for both the trend and the residual.

3.1. Trend model

For modelling the trend in the observed *Fulmaris glacialis* densities, we looked at the external variables of sea water depth and distance to the coast. Figure 4 shows that (i) average densities increased with increasing water depth, and that given water depth (ii) average densities increased with distance to coast in 1998, and slightly decreased with distance to coast in 1999.

For each year, a Poisson regression model (McCullagh and Nelder, 1989) fitted to the data was:

$$\begin{aligned} \mathrm{E}(y_t(s)) = \mu_t(s), \quad \log(\mu_t(s)) = \beta_{0,t} + \beta_{1,t}\mathrm{Depth}(s) + \beta_{2,t}\mathrm{Distance}(s), \\ s \in \{s_{1,t}, \ldots, s_{n_t,t}\},\ t \in \{98, 99\} \end{aligned} \tag{2}$$

It further assumes that variance is proportional to mean values:

$$\mathrm{Var}(y_t(s)) = \phi_t \mu_t(s) \tag{3}$$

with ϕ_t the over-dispersion parameter. The regression coefficients, as fitted for each year with the `glm` function in S-PLUS (using the `quasi` distribution family), are shown in Table 1. It should be noted here that the standard errors and t-values are of little value, as the spatial correlation of observations was ignored.

At unobserved locations s_0 and for a given time $t \in \{98, 99\}$, given the water depth and distance to coast (Figure 1) and given estimated coefficients $\hat{\beta}_0, \hat{\beta}_1$ and $\hat{\beta}_2$, the trend value is estimated by

$$\hat{\mu}_t(s_0) = \exp(\hat{\beta}_{0,t} + \hat{\beta}_{1,t}\mathrm{Depth}(s_0) + \hat{\beta}_{2,t}\mathrm{Distance}(s_0)) \tag{4}$$

In addition to the predicted value, Poisson regression yields a standard error for $\hat{\mu}_t(s_0)$, $\sigma_{\mu,t}(s_0)$. At observation locations, residuals can be calculated relative to the trend:

$$\hat{e}_t(s) = y_t(s) - \hat{\mu}_t(s), \quad s \in \{s_{1,t}, \ldots, s_{n_t,t}\}, t \in \{98, 99\} \tag{5}$$

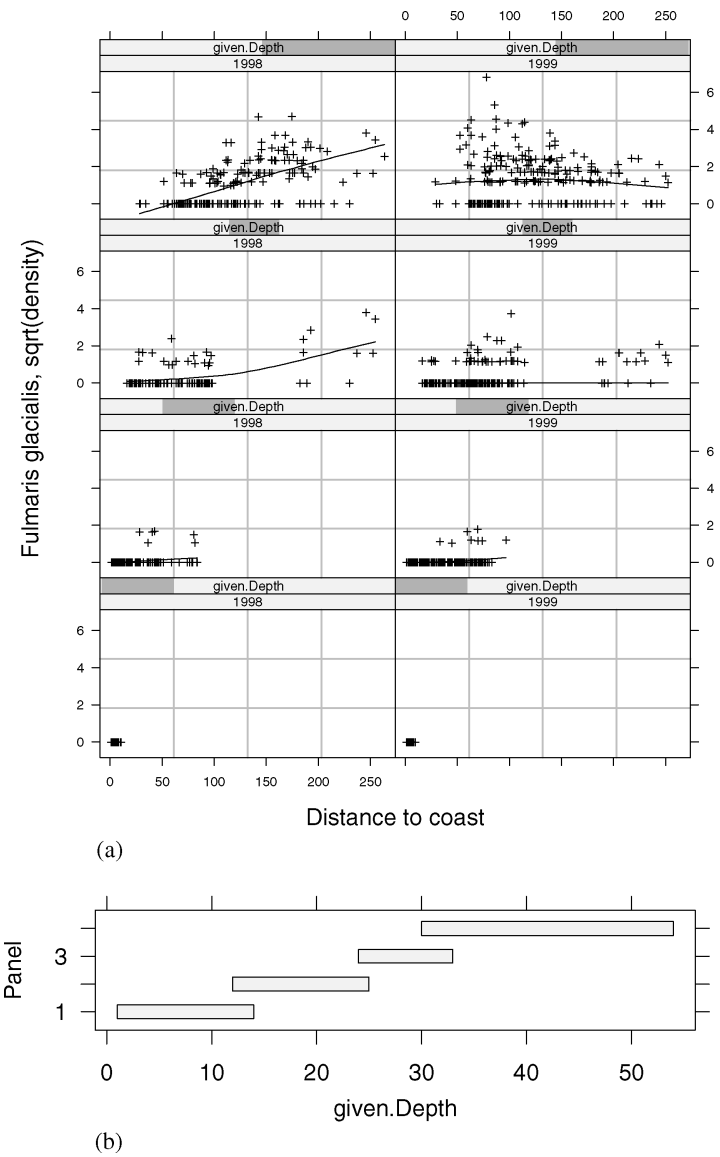

Figure 4. (a) Densities for *Fulmaris glacialis* as a function of year (left: 1998; right: 1999), distance to coast and sea water depth. Drawn lines denote a loess curve, fitted using standard settings of S-PLUS 6.0; (b) sea water depth classes for the four rows in (a). Densities were square-root transformed to stabilize their variance

3.2. Residual spatial correlation

As seen in (3), the variability in residuals is proportional to the mean value of y. For looking at spatial correlation, we transform residuals to Pearson residuals such that they have a constant variance ϕ_t:

$$r_t(s) = \frac{y_t(s) - \hat{\mu}_t(s)}{\sqrt{\hat{\mu}_t(s)}}, \quad s \in \{s_{1,t}, \ldots, s_{n_t,t}\}, \ t \in \{98, 99\} \tag{6}$$

Table 1. Poisson regression coefficients, their standard error and t-value, and dispersion parameters for the 1998 and 1999 trend models of *Fulmaris glacialis*. Note that standard errors and t-values assume independence, whereas the data are spatially dependent

Year	Parameter	Value	Std. error	t-value
1998	Intercept	−4.11	0.373	−11.03
	Depth	0.0685	0.00959	7.04
	Distance	0.0160	0.00123	12.99
	Dispersion	2.178		
1999	Intercept	−4.47	0.338	−13.22
	Depth	0.159	0.0112	14.24
	Distance	−0.00650	0.00201	−3.24
	Dispersion	3.83		

The residuals from the regression function do exhibit spatial correlation. The Pearson residual sample variograms,

$$\hat{\gamma}_t(\tilde{\boldsymbol{h}}) = \frac{1}{2N_{h,t}} \sum_{i=1}^{N_{h,t}} (\hat{\boldsymbol{r}}_t(s) - \hat{\boldsymbol{r}}_t(s+h))^2, \quad t \in \{98, 99\}, h \in \tilde{\boldsymbol{h}} \tag{7}$$

with $N_{h,t}$ the number of residual pairs in year t for distance class $\tilde{\boldsymbol{h}}$, calculated for distance intervals $\tilde{\boldsymbol{h}} = \{0 - 10000\text{m}, 10000 - 20000\text{m}, \ldots, 90000 - 100000\text{m}\}$ confirm this (Figure 5). In addition, the 1998 × 1999 sample cross-variogram (Clark *et al*., 1989; Cressie, 1993)

$$\hat{\gamma}_{98\times 99}(\tilde{\boldsymbol{h}}) = \frac{1}{2N_h} \sum_{i=1}^{N_h} (\hat{\boldsymbol{r}}_{98}(s) - \hat{\boldsymbol{r}}_{99}(s+h))^2, h \in \tilde{\boldsymbol{h}} \tag{8}$$

suggests that the residual patterns of both years are strongly cross-correlated. For modelling the variograms, we used exponential variogram functions, $\gamma(h) = c_0 + c_1(1 - \exp(-h/a))$, with c_0 the nugget, c_1 the partial sill and a the range parameter. The coefficients were fitted such that they (i) fitted the direct variograms best and (ii) complied to the linear model of coregionalization (Chilès and Delfiner, 1999). For our two-variable case, this model implies that: (i) the ranges are equal for all three variograms; (ii) $|c_{0,98\times 99}| \leq \sqrt{c_{0,98}c_{0,99}}$; and (iii) $|c_{1,98\times 99}| \leq \sqrt{c_{1,98}c_{1,99}}$. Table 2 shows the fitted variogram and cross-variogram coefficients and Figure 5 shows sample variograms and fitted models. Given this model for the spatial (cross)-correlation, we can spatially predict the residuals.

3.3. Residual spatial prediction

Although the symbols in Figure 3 cover a fair amount of the surface, the actual measurements together cover less than 1 per cent of the surface of NCP. We need to predict, or interpolate, the measurements in order to cover the remaining areas. For spatial prediction we simply add the estimated trend values $\hat{\mu}(s_0)$ (4) to the predicted residuals for a single year by

$$\hat{\boldsymbol{y}}_t(s_0) = \hat{\boldsymbol{\mu}}_t(s_0) + \hat{\boldsymbol{e}}_t(s_0), \quad t \in \{98, 99\} \tag{9}$$

and this subsection will explain how we predict $\hat{\boldsymbol{e}}_t(s_0)$.

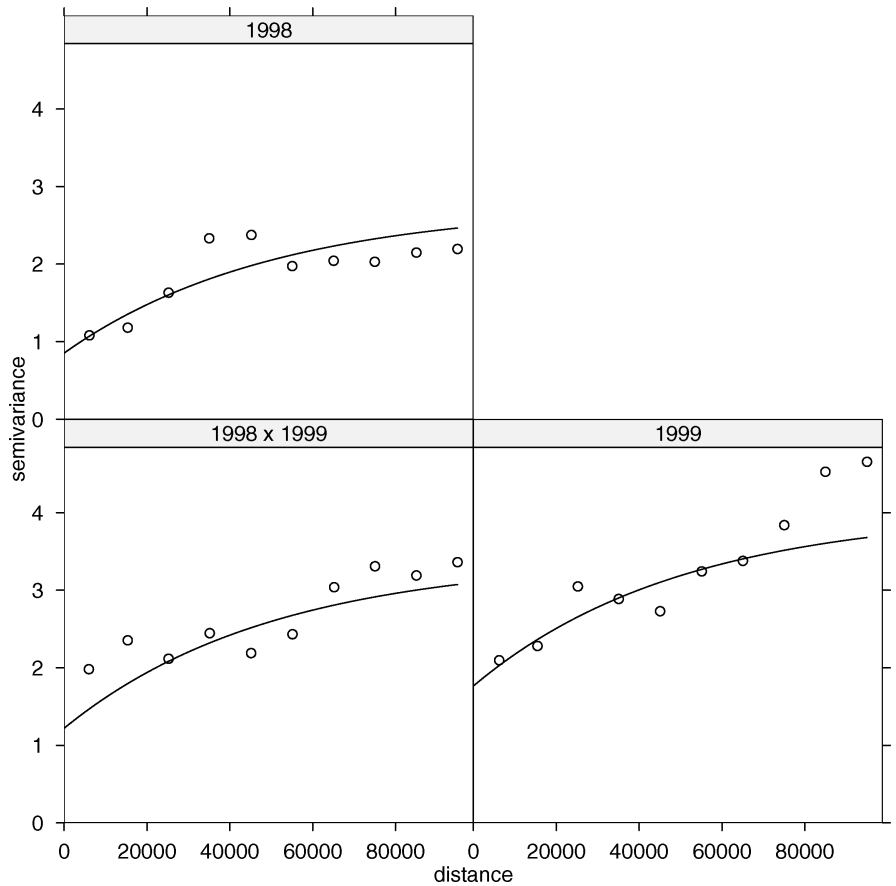

Figure 5. Residual variograms (top, lower right) and cross-variogram (lower left) for 1998 and 1999 residuals. Distance values plotted for symbols are average values for each distance interval

The first, simple approach is to use simple kriging (Cressie, 1993) for each year separately, to interpolate residuals (5) using the direct variograms of Figure 5. The second approach is to use simple cokriging (Cressie, 1993), which addresses the cross-correlation between residuals of both years shown in the cross-variogram of Figure 5: residuals for 1999 are used to predict residual values for 1998, and vice versa.

Table 2. Variogram (1998, 1999) and cross-variogram (1998×1999) model coefficients

Year	c_0	c_1	a
1998	0.85	1.89	50 000
1999	1.76	2.25	50 000
1998×1999	1.22	2.18	50 000

For the general simple cokriging case, suppose we have m time slices of observations, stacked in the vector $\mathbf{y}(s) = (y_1(s), \ldots, y_m(s))^{\mathrm{T}}$, with T denoting transpose, and we want to predict the $m \times 1$ vector $\mathbf{y}(s_0) = (y_1(s_0), \ldots, y_m(s_0))^{\mathrm{T}}$. The simple cokriging prediction is

$$\hat{\mathbf{y}}(s_0) = \hat{\mu}(s_0) + v' V^{-1}(y(s) - \hat{\mu}(s)) \tag{10}$$

with given $\hat{\mu}(s_0) = (\hat{\mu}_1(s_0), \ldots, \hat{\mu}_m(s_0))^{\mathrm{T}}$, and

$$v = \begin{bmatrix} v_{1,1} & v_{1,2} & \cdots & v_{1,m} \\ v_{2,1} & v_{2,2} & \cdots & v_{2,m} \\ \vdots & \vdots & \ddots & \vdots \\ v_{m,1} & v_{m,2} & \cdots & v_{m,m} \end{bmatrix}, V = \begin{bmatrix} V_{1,1} & V_{1,2} & \cdots & V_{1,m} \\ V_{2,1} & V_{2,2} & \cdots & V_{2,m} \\ \vdots & \vdots & \ddots & \vdots \\ V_{m,1} & V_{m,2} & \cdots & V_{m,m} \end{bmatrix}$$

where element i of the $(n_k \times 1)$ vector $v_{k,l}$ is $\mathrm{Cov}(y_k(s_i), y_l(s_0))$, and where element (i, j) of the $(n_k \times n_l)$ matrix $V_{k,l}$ is $\mathrm{Cov}(y_k(s_i), y_l(s_j))$. The corresponding simple cokriging prediction error covariance matrix is

$$\Sigma(s_0) = \Sigma_0 - v' V^{-1} v \tag{11}$$

where Σ_0 is the $m \times m$ matrix $\mathrm{Var}(\mathbf{y}(s_0))$. These equations reduce to the simple kriging equations when $m = 1$.

Both simple kriging and simple cokriging yield a prediction standard error $\sigma_{e,t}(s_0)$ for $\hat{e}_t(s_0)$. Only cokriging yields the full prediction error covariance, in our case providing $\mathrm{Cov}(\hat{e}_{98}(s_0), \hat{e}_{99}(s_0))$ (Ver Hoef and Cressie, 1993).

Given the proportionality of the variance of $e_t(s)$ given in (3), rather than using stationary covariances or semivariances, we prefer to use non-stationary covariances (Gotway and Stroup, 1997):

$$\begin{aligned} \mathrm{Cov}(y_k(s_i), y_l(s_j)) &= \sqrt{\mathrm{Var}(y_k(s_i))\mathrm{Var}(y_l(s_j))}\mathrm{Corr}(y_k(s_i), y_l(s_j)) \\ &\approx \sqrt{\hat{\phi}_k \hat{\mu}_k(s_i) \hat{\phi}_l \hat{\mu}_l(s_j)}\mathrm{Corr}(y_k(s_i), y_l(s_j)), \{k, l\} \in \{98, 99\} \end{aligned} \tag{12}$$

where the product of the correlations and dispersion coefficients are derived from Pearson residual variograms:

$$\sqrt{\hat{\phi}_k \hat{\phi}_l}\mathrm{Corr}(y_k(s_i), y_l(s_j)) = \sqrt{\hat{\phi}_k \hat{\phi}_l}\rho(h) = \gamma_{k \times l}(\infty) - \gamma_{k \times l}(s_i - s_j) \tag{13}$$

with $\rho_{p \times q}(h)$ the $(k \times l$ cross)-correlogram, and $\gamma_{p \times q}(\infty)$ the sill of either the cross-variogram (if $p \neq q$) or one of the direct variograms (if $p = q$).

Prediction standard errors for $\hat{y}_t(s_0)$ are approximated by combining the estimation error for the trend and the prediction (kriging) error for the residual:

$$\sigma_t(s_0) = \sqrt{\sigma^2_{\mu,t}(s_0) + \sigma^2_{e,t}(s_0)}, \; t \in \{98, 99\} \tag{14}$$

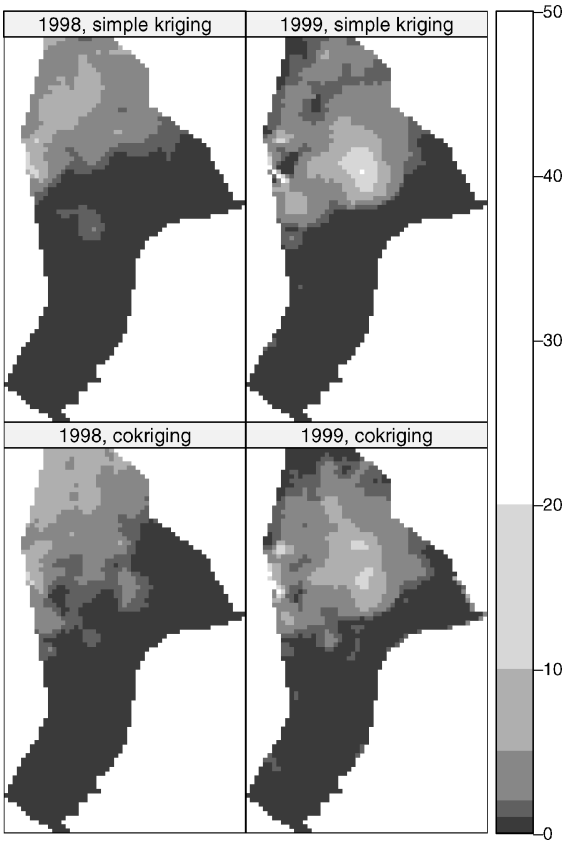

Figure 6. Predicted densities for *Fulmaris glacialis*, 1998 and 1999, simple kriging and cokriging

Figure 6 shows the predicted densities for *Fulmaris glacialis*, for August/September 1998 and 1998, as obtained by simple residual kriging and residual cokriging. Figure 7 shows the corresponding standard errors (14).

4. SPATIALLY AGGREGATED ESTIMATES

The high resolution maps of Figure 6 show a wealth of spatial patterns. The corresponding standard errors (Figure 7) are fairly high, however, because each prediction corresponds to an area the size of an individual measurement (point kriging). For larger areas predictions can be made by using block (co)kriging, predicting

$$y_t(B_0) = \frac{1}{|B_0|}\int_{B_0} y_t(u)\,\mathrm{d}u \tag{15}$$

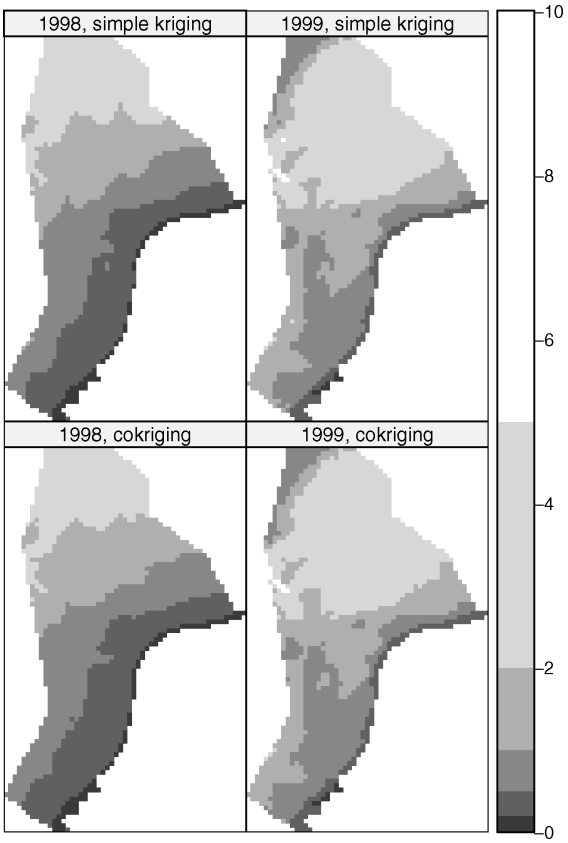

Figure 7. Standard errors of predicted densities for *Fulmaris glacialis*, 1998 and 1999, simple kriging and cokriging

with $|B_0|$ the area of B_0. We approximated $y_t(B_0)$ by averaging $\hat{\mu}_t(s)$ over block B_0, and by adding the simple block (co)kriging prediction $\hat{e}_t(B_0)$ to this. Block kriging proceeds by integrating the covariance functions over the block over which we aggregate, and yields standard errors $\sigma_t(B_0)$ for block aggregate predictions $\hat{y}_t(B_0)$; details are found in Journel and Huijbregts (1978) and Cressie (1993), for example.

A commonly used subdivision of the NCP into larger sub-areas is shown in Figure 8. Table 3 shows the block kriging predictions, along with their residual prediction standard errors (for this table, the estimation error of the block mean trend $\hat{\mu}_t(B_0)$ was not assessed).

5. TEMPORAL CHANGES

Besides spatial patterns and means, a main issue in monitoring is temporal change, and the detection of trends. We assessed location specific temporal changes in both high-resolution spatial patterns and in mean values for larger areas. Of special importance here is the prediction error of estimated temporal changes, which help indicate the significance of the temporal changes.

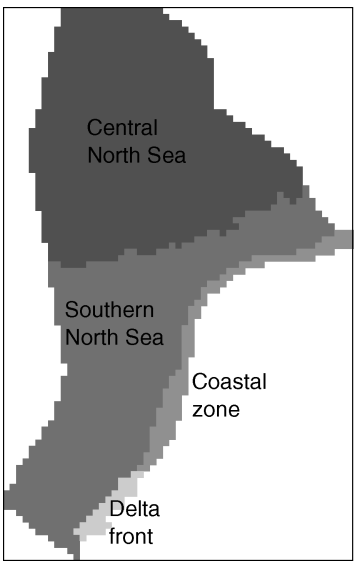

Figure 8. Subdivision of the NCP in large sub-areas

To assess temporal changes in sea bird densities from m temporal estimates at s_0, $\hat{\mathbf{y}}(s_0) = (\hat{y}_1(s_0), \ldots, \hat{y}_m(s_0)^{\mathrm{T}}$, we can estimate location-specific contrasts

$$\hat{C}(s_0) = \sum_{i=1}^{m} \lambda_i \hat{y}_i(s_0) = \lambda^{\mathrm{T}} \hat{\mathbf{y}}(s_0) \tag{16}$$

by suitably choosing λ. The standard error of this contrast $\hat{C}$ is $\lambda^{\mathrm{T}}\mathrm{Cov}(\hat{\mathbf{y}}(s_0))\lambda$, with $\mathrm{Cov}(\hat{\mathbf{y}}(s_0))$ the prediction error covariance matrix of $\hat{\mathbf{y}}(s_0)$, which is yielded by cokriging. For example, when we model the predicted values as changing linearly with time,

$$\hat{y}(s_0, t_i) = b_0(s_0) + b_1(s_0)t_i + \epsilon(s_0, t_i)$$

then λ can be chosen such that $\hat{C}$ estimates $b_1(s_0)$.

Table 3. Block average sea bird density estimates for the blocks of Figure 8 and their standard errors, obtained with simple kriging or simple cokriging; $\sigma_{res,1998}$ refers to the residual prediction error, for year 1998 (the standard error for the trend component was ignored for the results in this table)

	Simple kriging				Simple cokriging			
Area	$\hat{y}_{1998}$	$\sigma_{res,1998}$	$\hat{y}_{1999}$	$\sigma_{res,1999}$	$\hat{y}_{1998}$	$\sigma_{res,1998}$	$\hat{y}_{1999}$	$\sigma_{res,1999}$
Central North Sea	3.017	0.236	4.258	0.254	3.167	0.154	4.023	0.198
Southern North Sea	0.235	0.0462	0.350	0.0695	0.187	0.0336	0.444	0.0573
Coastal zone	0.00922	0.0227	0.0164	0.0401	0.00369	0.0178	0.0235	0.0328
Delta front	0.00298	0.0297	0.0144	0.0565	0.00290	0.0251	0.0114	0.0427

In our case, where we only consider $m = 2$ years, the contrast is the difference between years $C = \hat{y}_{99}(s_0) - \hat{y}_{98}(s_0)$, obtained by choosing $\lambda = (-1, 1)^{\mathrm{T}}$. In this case,

$$\mathrm{SE}_C = \sqrt{\mathrm{Var}(\hat{y}_{98}(s_0)) + \mathrm{Var}(\hat{y}_{99}(s_0)) - 2\mathrm{Cov}(\hat{y}_{98}(s_0), \hat{y}_{99}(s_0))}$$

An alternative but equivalent formulation for estimating differences using cokriging is given by Papritz and Flühler, 1994.

Figure 9 shows estimated differences and standard errors for *Fulmaris glacialis*, both obtained by cokriging (using (16)) and by simple kriging. In this figure, the simple kriging difference standard errors were obtained by $\sqrt{\sigma^2_{98}(s_0) + \sigma^2_{98}(s_0)}$, thus ignoring residual correlations between years. Figure 10 shows where the absolute differences are larger than twice their standard error, indicating areas where the estimated differences are unlikely to be attributed to mere chance.

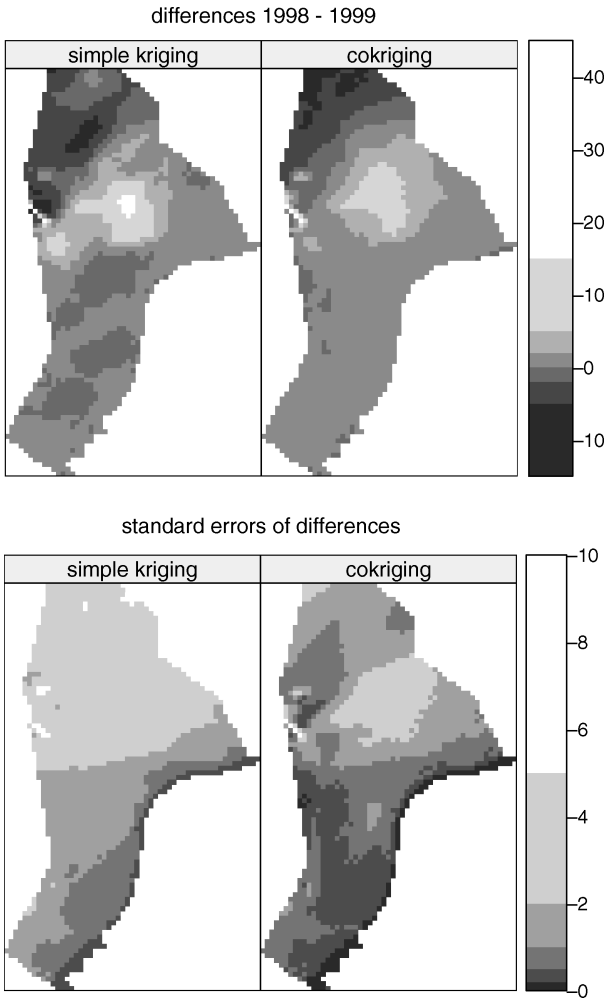

Figure 9. Estimated differences (top) and standard errors of differences (bottom) for *Fulmaris glacialis* using simple kriging and cokriging

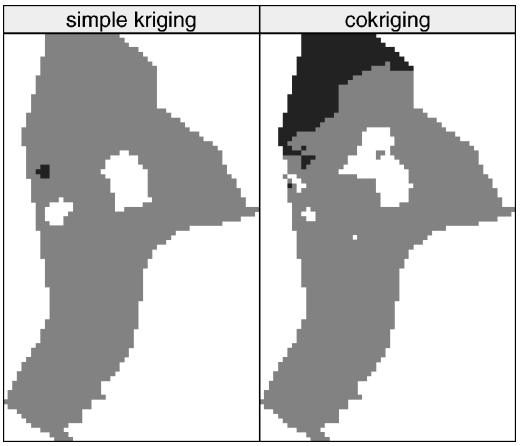

Figure 10. Classified differences: if $\hat{C} < -2\text{SE}$ a difference is classified as a decrease (white), if $\hat{C} > 2\text{SE}$ a difference is classified as an increase (black), remaining cells are classified as not significantly changing (grey). Left: using simple kriging predictions and standard errors, right: using cokriging predictions and standard errors (Figure 9)

6. RESULTS

Figure 6 shows densities for *Fulmaris glacialis*, estimated using simple kriging and cokriging. The predicted pattern confirms the species' preference for open sea, a pattern that is evident when glancing at Figure 3. Figure 7 shows prediction standard errors. Prediction errors increase when predicted values increase: a consequence of proportionality of variance (3). For most of the area the cokriging prediction errors are smaller than those obtained by simple kriging. This is no surprise given the strong correlation between the two years studied (Figure 5), which gives each year's observations considerable weight for the prediction of densities in the other year. Figure 9 shows predicted differences for 1998–1999 and their standard errors. Both methods yield a similar global pattern; cokriging results in significantly (2–3 times) smaller standard errors. Figure 10 shows classified difference, indicating predicted differences that exceed twice their standard error; here, cokriging reveals many more trends.

Tables 4 and 3 show that averaged over large areas in 1999 the number of *Fulmaris glacialis* in the NCP is significantly larger than in 1998, where significance is indicated by the notion that the estimated difference exceeds twice its standard error. For the temporal differences of Table 4, cokriging and simple kriging lead to different, but not necessarily conflicting estimates, and cokriging estimates have standard errors that are 2–3 times smaller than those obtained by simple kriging.

Table 4. Block mean estimates of differences for the areas shown in Figure 8, using simple kriging or cokriging; SE_C refers to the prediction error (the standard error for the trend component was ignored for the results in this table)

	Simple kriging		Cokriging	
Area	$\hat{C}$	SE_C	$\hat{C}$	SE_C
Central North Sea	1.241	0.347	0.856	0.106
Southern North Sea	0.1150	0.0835	0.2569	0.0367
Coastal zone	0.00722	0.0461	0.0198	0.0216
Delta front	0.0114	0.0638	0.00848	0.0266

7. DISCUSSION AND CONCLUSIONS

This article presents block average densities and temporal changes in sea bird densities for *Fulmaris glacialis* in 1998 and 1999, and it illustrates a simple approach to interpolation that combines generalized linear modelling for the trend with geostatistical modelling of the residual that extends the work of Gotway and Stroup (1997). The trend model is log-linear (2) in distance to coast and sea floor depth; the residual model uses simple (block) cokriging (10) with residual (co)variances that are proportional to the mean response (3), (12), (13).

The approach taken matches the observations and the processes considered, as it yields positive estimates of the trend, and flexible modelling of the trend function is allowed. The approach yields reasonable estimates (i.e. the spatial trend function) in regions where data are sparse, and in location-specific, data-driven predictions of deviations from the trend function in areas where observations suggest such deviations. Furthermore, prediction standard errors are provided for point estimates, block mean estimates, and for temporal differences in both.

A number of important aspects may have been missed, however. From an ecological point of view, the variables that were taken as covariates may not be the preferred ones. Better variables would address the behaviour of the animals more directly, and should for instance be related to feeding habits (e.g. availability of fish or shellfish species), and breeding (e.g. distance to breeding colonies). Only very general information (coast aversion, relation of food to water depth) is carried by the covariates currently used. Still, non-linear transformation or even more complex functions (higher order polynomials or interactions) might be considered for the two covariates used here.

For the case presented here, it matters a great deal whether prediction errors between years are considered independent (e.g. for reasons of convenience) or dependent. The latter assumption requires the use of cokriging to assess kriging predictions, prediction error variances and prediction error covariances. Because the residual spatial patterns for 1998 and 1999 were strongly positively correlated, calculating the difference between the predictions for years 1999 and 1998 largely decreases the prediction standard error of the difference when prediction error covariances are taken into account. Using cokriging to assess changes between two moments in time not only results in a more realistic framework with respect to the underlying assumptions, but also results in standard errors for the differences that are 2–3 times smaller than the simple kriging standard errors; larger areas can be said to be significantly different than for the case where temporal dependence was ignored (i.e. simple kriging). Also, for the block aggregate estimates for the areas of Figure 8, cokriging yielded more significant changes than simple kriging (Table 3). Compared to simple kriging, standard errors for differences obtained with cokriging were lower by a factor of 2–4 (Table 3). It is shown that the approach taken here allows the assessment of location specific estimates of gradual change over multiple years.

Negative density estimates (Table 3) are an artifact of the residual interpolation procedure used here: spatial trends are treated on the log-scale and cannot become negative when back transformed, but residuals are predicted on the observation scale and cannot be guaranteed to yield a positive density estimate when added to the trend estimate. For the case considered here, the negative values are all very close to zero, and the estimation errors exceed their values by some factors. The approach proposed by Diggle *et al*. (1998) would solve this issue. Applying their approach would, however, require specification of prior distributions on all coefficients, and at the time of writing this article the procedure was computationally too demanding for data sets the size of the one used here.

The presence of measurement errors in the data have not been addressed here. They may include systematic errors (birds are more easily missed when small waves are present, when they occur in

many small groups, or when light or wave conditions are suboptimal), or random errors (large groups are estimates rather than counted exactly). Also, for the interpolation step we assumed that the spatial field did not change between the three flight dates.

For the estimation of trend coefficients, spatial and temporal correlation in observations was ignored. Pebesma *et al*. (2000a, 2000b) dealt with this issue by using a generalized estimating equation approach (Liang and Zeger, 1986; Zeger and Liang, 1986), but encountered recurring problems with convergence of regression and variogram coefficients.

The following simplifying assumptions were made and need mentioning: (i) during the estimation of spatial correlation (3.2) the residuals were treated as regular observations (correlation resulting from subtracting a common, estimated trend was ignored); (ii) no variance functions other than that of (3) were considered (e.g. the negative binomial would have been a viable alternative); and (iii) we did not consider anisotropy (direction dependent spatial correlations), because the data are collected along linear flight paths. These issues lead to a potential bias and underestimation of uncertainties.

ACKNOWLEDGEMENTS

The authors acknowledge the help of Cor Berrevoets, Floor Arts, and Ana Bio. RIKZ supported the development of the gstat R package, an open source project used for this study. The data and R or S-PLUS script files used are available from the first author's web-site.

REFERENCES

Chilès JP, Delfiner P. 1999. *Geostatists, Modelling Spatial Uncertainty.* Wiley, New York, 695 pp.

Clark I, Basinger KL, Harper WV. 1989. Muck—a novel approach to cokriging. In *Proc. Conf. on Geostatistical, Sensitivity, and Uncertainty Methods for Ground Water Flow and Radionuclide Transport Modeling*, Buxton BE (ed.), San Francisco, CA, 15–17 Sept 1987. Battelle Press: Columbus; 473–493.

Cressie NAC. 1993. *Statistics for Spatial Data*, Revised Edition. Wiley: New York.

Diggle PJ, Tawn JA, Moyeed RA. 1998. Model-based geostatistics. *Applied Statistics* **47**(3): 299–350.

Gotway CA, Stroup WW. 1997. A generalized linear model approach to spatial data analysis and prediction. *Journal of Agricultural, Biological and Environmental Statistics* **2**(2): 157–178.

Heuvelink GBM, Pebesma EJ. 1999. Spatial aggregation and soil process modelling. *Geoderma* **89**: 47–65.

Journel AG, Huijbregts ChJ, 1978, *Mining Geostatistics*. Academic Press: London.

Liang K-Y, Zeger SL. 1986. Longitudinal data analysis using generalized linear models. *Biometrika* **73**(1): 13–22.

McCullagh P, Nelder JA. 1989. *Generalized Linear Models*, 2nd edn. Chapman & Hall: London.

Papritz A, Flühler H. 1994. Temporal change of spatially autocorrelated soil properties: optimal estimation by cokriging. *Geoderma* **62**: 29–43.

Pebesma EJ, de Kwaadsteniet JW. 1997. Mapping groundwater quality in the Netherlands. *Journal of Hydrology* **200**: 364–386.

Pebesma EJ, Bio AMF, Duin RNM. 2000a. Mapping sea bird densities on the North Sea: combining geostatistics and generalised linear models. In *Geostatistics 2000 Cape Town. Proceedings of the Sixth International Geostatistics Congress held in* Cape Town, South Africa, April 2000, Kleingeld WJ, Krige DG (eds). Vol. 2, 654–663.

Pebesma EJ, Duin RNM, Bio AMF. 2000b. *Spatial Interpolation of Sea Bird Densities on the Dutch Part of the North Sea*. ICG report 00/10, Utrecht University.

Ver Hoef JM, Cressie NAC. 1993. Multivariable spatial prediction. *Mathematical Geology* **25**(2): 219–240.

Zeger SL, Liang K-Y. 1986. Longitudinal data analysis for discrete and continuous outcomes. *Biometrics* **42**: 121–130.

